Annual Report 2008

08151: Finite fault parameterization of intermediate and large earthquakes in Southern California

Chen Ji (UCSB)

Finite fault parameterization of intermediate and large earthquakes in Southern California

The quick finite fault algorithm, which is currently used to monitor the global large earthquakes, is adopting to routinely study finite fault parameters of the mediate and large earthquakes in Southern California using the CISN realtime dataset.

Since this technique has already been demonstrated for the study of large earthquakes, during 2008 our research focused on the feasible data process and inverse schedules for the study of the moderate earthquakes. To study the moderate earthquake, we need use the higher frequency seismic waveforms, which is very sensitive to the 3D earth structure. *Tan and Helmberger* [2007] pointed out that the high frequency P waveforms (0.5-2Hz) recorded at LA basin could be modeled using 1D Green's functions after adding path-dependent time shifts and multiplying amplitude amplification factors (AAFs). They defined the AAFs as the amplitude ratios between records of a calibration event and the corresponding 1D synthetics, and found that the AAFs are relatively stable and mechanism independent [*Tan and Helmberger*, 2007]. However, a good calibration event may not always be available. So we have attempted to define them using state-of-art 3D SCEC-CVM models**.** 2008 Chino Hills earthquake was used as the test event.

1. **Estimating path-dependent time shifts using 3D velocity structure is not feasible**. The arrival-times predicted by 3D velocity structure are much better than the 1D predictions, but the errors are still up to half second. Considering the typical source duration of moderate earthquakes, this technique is not appropriate to study these events. We instead to resolve this issue by aligning the observations and synthetics with their first arrivals. However, this technique is still plausible when we study large earthquakes.
2. **Estimating P wave AAFs by comparing 3D and 1D synthetic seismograms is plausible**. We have estimated synthetic AAFs as the amplitude ratios between 3D and 1D synthetics calculated using the main-shock moment tensor solution. We adopt the SCEC CVM-H model and the Spectral Element Method [*Komatitsch et al.*, 2004] to generate the 3D synthetics. Figure 1 shows the comparison of waveforms. The P-wave AAF corrections apparently correlate with the surface geology and change by a factor of 4 from 0.9 to 3.5 among the selected stations (Figure 1). As shown in Figure 2, after these corrections, the synthetic P waves match data very well. However, the predicted S wave AAF corrections appear to have large errors.
3. **Finite fault effect of a moderate earthquake in predicting 2-sec ground motion is nontrivial:** Figure 4 shows the comparisons among observed 2-sec peak ground velocity (PGV) map (Figure 4a) and synthetic maps based on point sources and two finite faults. Because the depth of rupture zone is 4-5 times of the dimension of the fault, even a point source reproduces the general pattern of PGV observations (Figure 4b). Note that ignoring the source finiteness overestimate the PGVs, particularly in the region right above the source. This should be considered in the future structure studies.

Publication that resulted from our activity related to this project is

(1) Shao, Guangfu, C. Ji and E. Hauksson, Rupture process and dynamic implications of the July 29, 2008 Mw 5.4 Chino Hills, California Earthquake, BSSA, 2009. submitted. SCEC # 1262

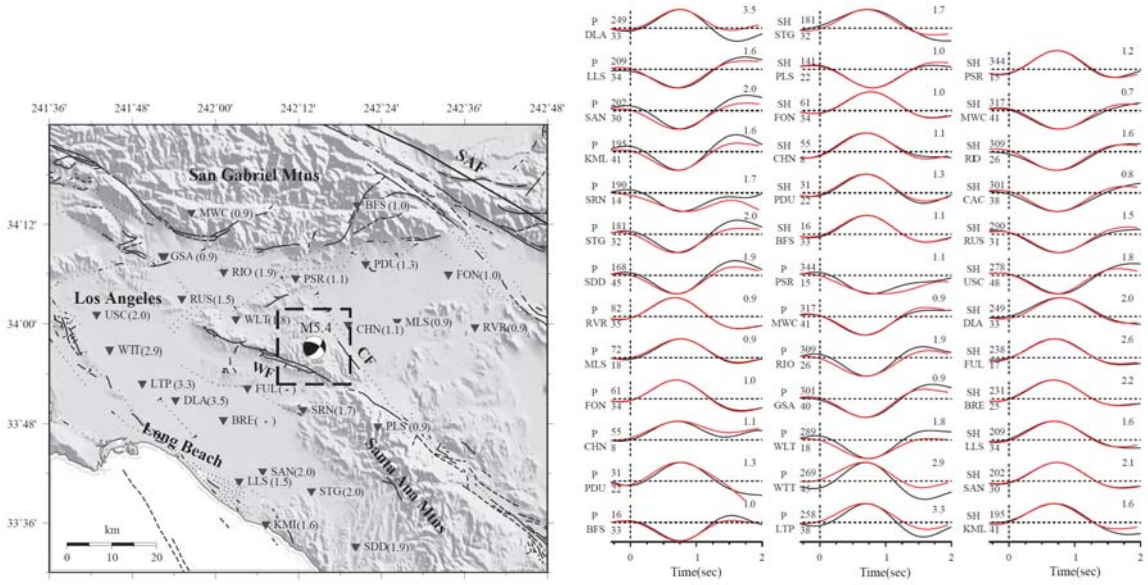

Figure 1. Left: Focal mechanism and location map of the 2008 Mw 5.4 Chino Hills earthquake. Triangles represent 26 seismic stations used in this study. The solid and dashed lines indicate the major fault traces in this area [*Jennings*, 1994] (SAF-San Andreas Fault; WF-Whittier Fault; CF-Chino Fault). The values inside parentheses indicate the P-wave AAFs derived from 3D to 1D comparisons shown in right. Note that we didn't get the AAFs at stations FUL and BRE because the waveforms of their 3D P-wave synthetics are significantly different with their 1D synthetics. Right: Comparison of 1D (red) and 3D (black) synthetic waveforms (0.16 – 1.0 Hz). They have been normalized by their peak amplitudes and aligned using a waveform cross-correlation procedure. The peak amplitude ratio (3D/1D) is denoted at the end of each trace, labeling as the AAFs in the left Figure. The number above the beginning of each trace is the source azimuth in degree and below is the epicentral distance in km.

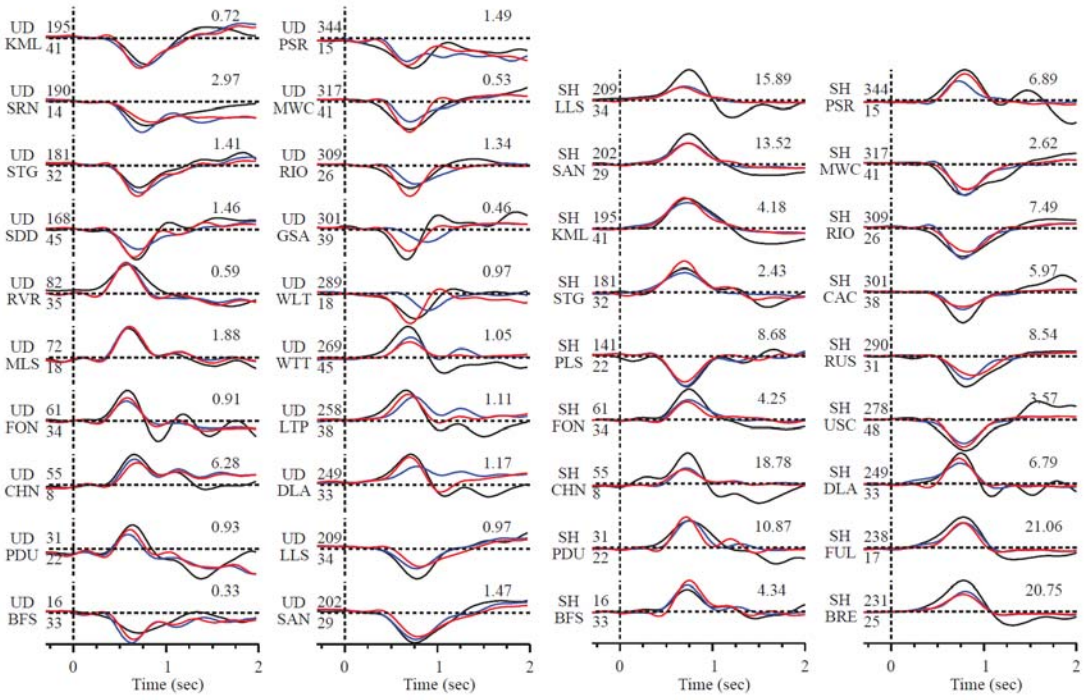

Figure 2. Comparison of observations (black traces) and synthetic seismograms calculated using the **Model I** (red traces) and the **Model II** (blue traces), fault models based on two nodal planes inferred from the moment tensor solution. Both data and synthetics are aligned on P or SH arrivals. All the waveforms have been filtered between 0.16 Hz and 2.5 Hz. The number at the end of each trace is the observed peak amplitude in millimeter. The number above the beginning of each trace is the source azimuth in degree and below is the epicentral distance in km. Note that the Model I significantly outperforms the Model II and has been identified as causative fault plane.

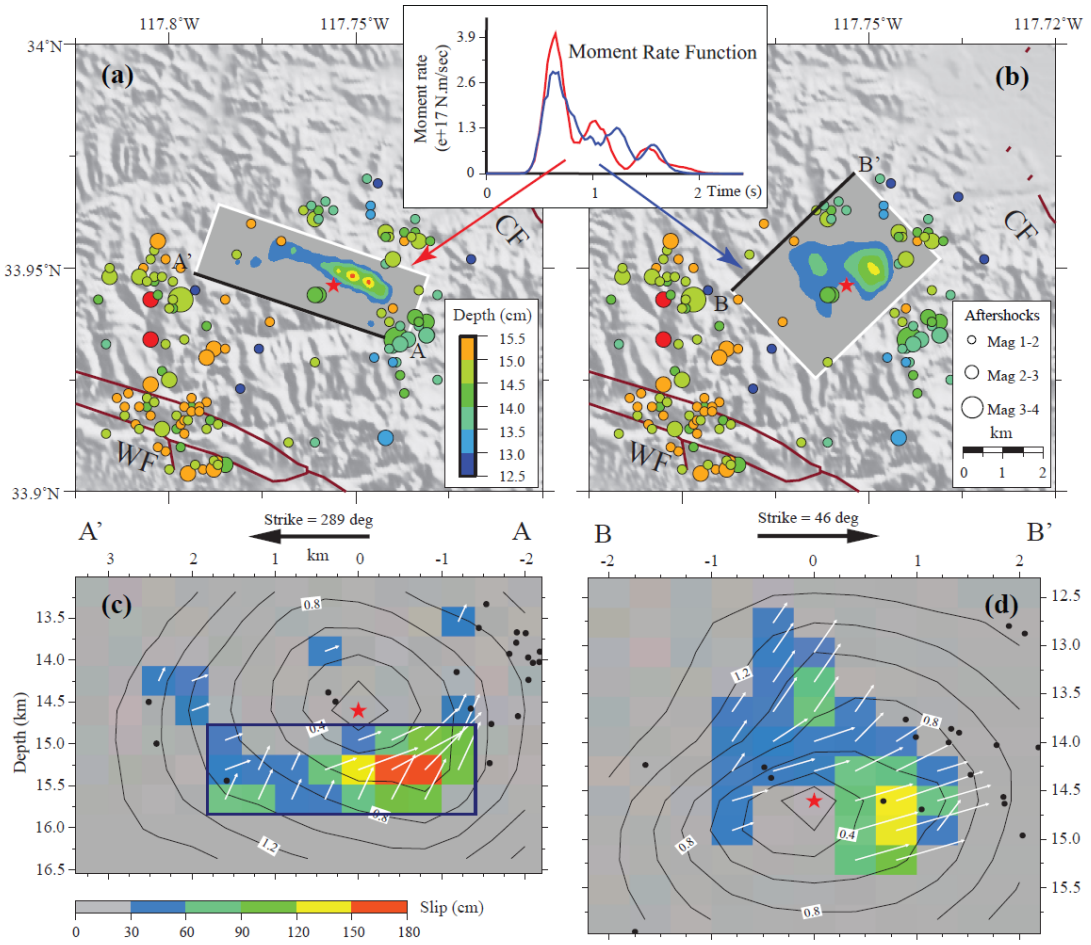

Figure 3. Comparison of inverted finite fault models based on two nodal planes (Table 1). (a) Surface projection of the Model I (white box) superimposed on the shaded relief. The red star indicates the epicenter of the mainshock. Black line A-A' indicates the top edge of the fault plane. Circles represent relocated aftershocks [*Hauksson et al.*, 2008] during the first month, with filled color denoting their hypocenter depth, and the radius indicating their magnitudes. WF-Whittier Fault; CF-Chino Fault. (b) Same as (a) but for Model II (c) Vertical cross-section of slip distribution of Model I. The black arrow indicates the fault strike and the red star denotes the hypocenter location. For each subfault, the color shows its dislocation amplitude and the arrow indicates the motion direction of the hanging wall relative to the footwall. The high slip region was outlined by a blue box. Black contours show the rupture initiation time in an interval of 0.2 s. Black dots denote the selected aftershocks located within 1 km of the fault plane (d) Similar to (c) but for Model II. Inserted figure compares the moment rate functions of Model I (red line) and Model II (blue line).

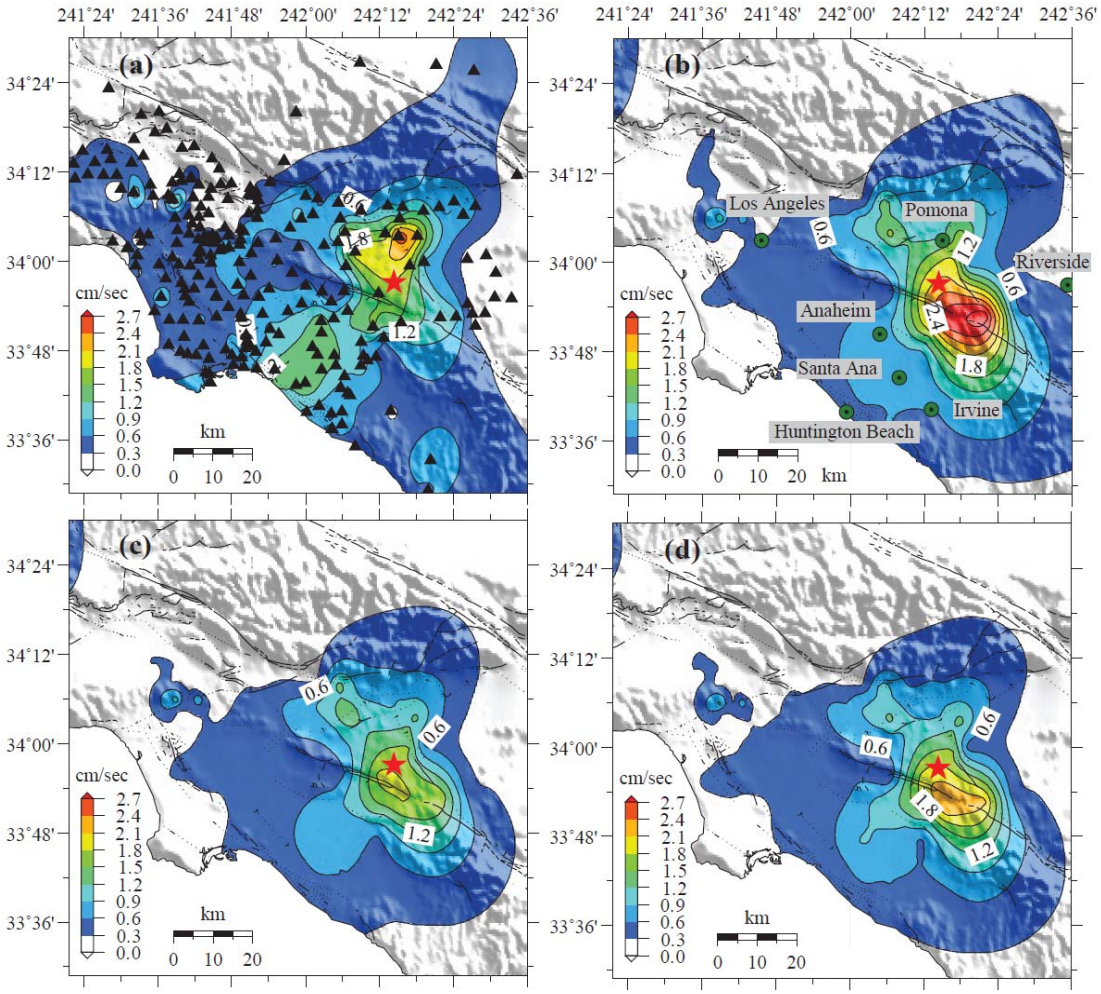

Figure 4. Comparison of PGV distributions (3sec-2sec). (a) Observed PGV map of the 2008 Mw 5.4 Chino Hills earthquake derived by interpolating the strong motion data at CISN and CGS stations (black triangles). (b) Spectral element method synthetic PGV map calculated using the point source (Table 1) and the SCEC CVM-H model. (c) SEM PGV map based on the Model I (Figure 2a). (d) SEM PGV map based on the Model II (Figure 2b).

References:

Hauksson, E., et al. (2008), Preliminary Report on the 29 July 2008 Mw 5.4 Chino Hills, Eastern Los Angeles Basin, California, Earthquake Sequence, *Seismological Research Letters*, *79*(6), 855-866.

Jennings, C. W. (1994), Fault activity map of California and adjacent areas: California Department of Conservation, Division of Mines and Geology, Geologic Data Map No. 6, scale 1:750,000.

Komatitsch, D., et al. (2004), Simulations of ground motion in the Los Angeles basin based upon the spectral-element method, *Bulletin of the Seismological Society of America*, *94*(1), 187-206.

Tan, Y., and D. Helmberger (2007), A new method for determining small earthquake source parameters using short-period P waves, *Bulletin of the Seismological Society of America*, *97*(4), 1176-1195.